Biochimica et Biophysica Acta 1838 (2014) 2910–2918

Contents lists available at ScienceDirect

Biochimica et Biophysica Acta

journal homepage: www.elsevier.com/locate/bbamem

Lipopolysaccharide induces amyloid formation of antimicrobial peptide HAL-2

Jiarong Wang, Yan Li, Xiaoming Wang, Wei Chen, Hongbin Sun *, Junfeng Wang *

High Magnetic Field Laboratory, Hefei Institutes of Physical Science, Chinese Academy of Science, Hefei, Anhui 230031, PR China

ARTICLE INFO

Article history:
Received 1 March 2014
Received in revised form 1 July 2014
Accepted 30 July 2014
Available online 7 August 2014

Keywords:
Antimicrobial peptide
HAL-2
NMR spectroscopy
Aggregation
Amyloid formation

ABSTRACT

Lipopolysaccharide (LPS), the important component of the outer membrane of Gram-negative bacteria, contributes to the integrity of the outer membrane and protects the cell against bactericidal agents, including antimicrobial peptides. However, the mechanisms of interaction between antimicrobial peptides and LPS are not clearly understood. Halictines-2 (HAL-2), one of the novel antimicrobial peptides, was isolated from the venom of the eusocial bee *Halictus sexcinctus*. HAL-2 has exhibited potent antimicrobial activity against Gram-positive and Gram-negative bacteria and even against cancer cells. Here, we studied the interactions between HAL-2 and LPS to elucidate the antibacterial mechanism of HAL-2 in vitro. Our results show that HAL-2 adopts a significant degree of β-strand structure in the presence of LPS. LPS is capable of inducing HAL-2 amyloid formation, which may play a vital role in its antimicrobial activity.

1. Introduction

Antibiotics have revolutionised the treatment of common bacterial infections. However, the widespread and frequent intake of antibiotics in small doses constitutes a constant selective pressure on pathogens and results in antibiotic-resistant strains [1]. Antibiotic resistance is the ability of a microorganism to withstand the effects of an antimicrobial agent as a result of chromosomal changes or the exchange of genetic material via plasmids and transposons [2]. This genetic variability of pathogens is a serious threat to public health, thereby creating a continuous need to develop new antibiotics.

Antimicrobial peptides (AMPs) are evolved host defence effector molecules that are produced by a wide variety of organisms, ranging from prokaryotes to humans [3–5]. AMPs possess an unusually broad spectrum of activity and are promising candidates for the development of therapeutic drugs in the fight against resistant pathogens [6–9]. The antibiotic action of most of AMPs stems from their ability to make the membrane permeable, though that may not be their sole mode of action [8,10,11]. Despite their diverse origins, AMPs share a common characteristic of harbouring small, positively charged, amphipathic structures [12,13]. The net cationicity and amphipathicity of AMPs mediates the interaction between AMPs and the highly anionic lipopolysaccharide (LPS) of Gram-negative bacteria, which constitutes the lipid portion of the outer membrane; this interaction causes the leakage of essential cell contents by forming pores or disturbing the lipid organisation [14–16]. It has been reported that many AMPs are able to neutralise the endotoxic effect of LPS on immune cells [17–20]. Therefore, studies on the structure of AMPs and their interactions with LPS are vital to improve our understanding of the antibacterial mechanisms of AMPs and to help design new antimicrobial peptides for therapeutic purposes.

A large number of AMPs have been derived from toxin-related polypeptides, such as the animal venoms from scorpions [21], spiders [22], bees [23], and snakes [24]. Due to their different mechanisms of action and incredible versatility, they have demonstrated an interesting alternative for controlling microorganisms that are resistant to conventional antibiotics. Halictines-2 (HAL-2, Gly-Lys-Trp-Met-Ser-Leu-Leu-Lys-His-Ile-Leu-Lys-NH2) is one of the shortest cationic AMPs isolated from the venom of the wild eusocial bee *Halictus sexcinctus* [25]. It has been reported that HAL-2 is active against Gram-positive and Gram-negative bacteria, the yeast pathogen *Candida albicans*, and has sufficient potency to kill several types of cancer cells.

The aim of this work was to study the molecular mechanism of HAL-2 antimicrobial activity. We focused on the interactions between HAL-2 and LPS, the Gram-negative bacterial cell wall barrier that broad-spectrum AMPs are able to break. The interaction of HAL-2 with LPS was investigated using various physicochemical methods, including circular dichroism (CD), nuclear magnetic resonance (NMR), surface plasmon resonance (SPR) and Thioflavin T (ThT) fluorescence. Our results show that HAL-2 interacts with LPS lipid and adopts a significant degree of β-strand structure to form amyloid aggregates. In comparison to HAL-2, three analogues that form less amyloid lost most of their antimicrobial activity. These results strongly suggest that the HAL-2 amyloid aggregates induced by LPS contribute to its antimicrobial activity.

* Corresponding authors. Tel.: +86 551 65591672, +86 551 65595669.
E-mail addresses: hbsun@hmfl.ac.cn (H. Sun), junfeng@hmfl.ac.cn (J. Wang).

http://dx.doi.org/10.1016/j.bbamem.2014.07.028
0005-2736/

2. Materials and methods

2.1. Peptide preparation

Synthetic antimicrobial peptide HAL-2 (GKWMSLLKHILK) and its analogues HAL-2L6(D) (GKWMSL(D)LKHILK), HAL-2K8P (GKWMSLLPHILK) and HAL-2H9P (GKWMSLLKPILK) were commercially provided by GL Biochem Ltd (Shanghai, China). The purity of the synthetic peptide used to evaluate biological activity was higher than 95%. Based on the amino acid sequence of HAL-2, the gene sequence encoding HAL-2 was synthesised by Genscript (Nanjing, China). Then, the HAL-2 gene was cloned into a modified vector pET22b to produce sumo fusion protein, and the cloning was verified by DNA sequencing. The peptide used for NMR studies was expressed in *Escherichia coli* BL21(DE3)/pLysS cells grown on minimal M9 medium supplemented with [^{15}N]ammonium chloride (Cambridge Isotope Laboratories). The fusion protein containing the peptide was affinity purified from the clarified supernatant with Ni^{2+}-NTA agarose resin (GE healthcare), and it was purified to homogeneity by fast protein liquid chromatography (GE healthcare). After cleavage by sumo-enzyme, the peptide was purified by reverse-phase HPLC (Bio-Rad, America) using a C18 semi-preparative column (Waters), and it was then lyophilised and analysed by ESI-MS.

2.2. Assessment of cell viability

In vitro time viability loss curves for HAL-2 were determined. Exponentially growing *E. coli* ATCC 25922 cells were resuspended in buffer at pH 7.4 (20 mM Tris, 100 mM NaCl) to obtain a density of 2×10^8 cfu/mL. The bacterial suspensions were incubated at 37 °C for increasing time intervals (from 20 to 180 min) with HAL-2 at concentrations of 20, 40, and 60 μM. After incubation, samples (10 μL) were removed from each well and diluted appropriately in buffer. Colony-forming units (CFUs) were determined by spotting 20 μL of serial dilution samples onto Mueller-Hinton agar plates, with an 18-hour incubation at 37 °C. For HAL-2 analogues, the bacterial suspensions were incubated at 37 °C for 180 min with peptides at concentrations of 60 μM.

2.3. Flow cytometry analysis

The effects of HAL-2 on bacterial membrane integrity were determined. In brief, *E. coli* ATCC 25922 cultures were resuspended at 2×10^8 cfu/mL in 1 mL buffer at pH 7.4 (20 mM Tris, 100 mM NaCl). The HAL-2 was added at concentrations of 20, 40, and 60 μM, and the samples were incubated at 37 °C for 180 min. The bacterial cells were harvested by centrifugation, resuspended in 1 mL buffer and incubated for 30 min in the dark at room temperature with PI (5 μg/mL final concentration, Sigma, USA). Flow cytometry (Becton–Dickinson) measurements were performed immediately thereafter.

2.4. Scanning electron microscopy (SEM)

The morphology changes induced by peptide HAL-2 on *E. coli* ATCC 25922 were studied using scanning electron microscopy, according to a modified procedure adapted from Wei et al. [26]. Accordingly, bacteria were resuspended at 2×10^8 cfu/mL in buffer at pH 7.4 (20 mM Tris, 100 mM NaCl) and incubated at 37 °C for 180 min with HAL-2 at different concentrations (20, 40, 60 μM). Then, an aliquot (10 μL) of each sample was serially diluted and plated onto Mueller-Hinton agar for a CFU count. The remaining bacterial cells were centrifuged at 8000 rpm for 5 min, and the pellet was fixed with 2.5% glutaraldehyde in PBS (pH 7.4) for 2 h at room temperature. After two washes with phosphate buffer saline (PBS), the cells were postfixed with 2% (w/v) $AuCl_3 \cdot HCl$ for 2 h, dehydrated in a graded series of ethanol, exchanged ethanol with tert-butyl alcohol; this mixture was then deposited on silicon wafers, frozen in liquid nitrogen, and then vacuum-dried overnight. After gold-plating and mounting onto aluminium stubs, the samples were analysed with Helios NanoLab™ 600i SEM following the manufacturer's instruction.

2.5. Circular dichroism (CD) spectroscopy

Circular dichroism (CD) experiments were carried out on a Jasco J-810 spectropolarimeter (Tokyo, Japan). The CD spectra of the HAL-2 and its analogues were recorded at room temperature from 190 to 240 nm. CD spectroscopy was used to investigate the secondary structure adopted by HAL-2 and its analogues in the absence and presence of LPS (2 mg/mL) from *E. coli* 055:B5 (Sigma). Peptides were dissolved at 0.2 mg/mL in buffer at pH 7.4 (20 mM Tris) for all CD experiments. The spectra were collected as averages over three scans using a 1-mm path length cell. A 1 nm data pitch, 100 nm/min scanning speed, 1 s response time and 1 nm bandwidth were generally used.

2.6. Nuclear magnetic resonance (NMR) spectroscopy

NMR experiments were recorded at 298 K on a 500 MHz Bruker spectrometer (Germany) equipped with a cryo-probe and pulse field gradients. 2D ^{1}H/^{15}N HSQC spectra were acquired on samples of uniformly 1 mM ^{15}N-labelled HAL-2 in the absence or presence of 0.05, 0.5, 1 mg/mL LPS. The experiments were performed in 20 mM Tris (pH 7.4), 100 mM NaCl. All spectra were processed and analysed by using the spectral processing and analysis systems NMRPipe and Sparky.

Interactions of HAL-2 with LPS were also examined by recording a series of one-dimensional ^{31}P NMR spectra of LPS at 298 K, whereby 4 mg/mL LPS in 20 mM Tris (pH 7.4), 100 mM NaCl was titrated with various concentrations (0.1, 0.2, 0.4, 0.8 and 1.0 mM) of peptide from a stock solution that was prepared in buffer at pH 7.4. The ^{31}P NMR spectra were recorded on a Bruker 850 MHz spectrometer equipped with ^{31}P direct-detection channel.

2.7. Surface plasmon resonance (SPR) experiments

The real-time binding interaction between HAL-2 and LPS was measured by SPR using a Biacore 3000 instrument (GE Healthcare) at 25 °C. The peptide was covalently immobilised on the certified grade CM5 sensor chips at concentrations of 0.2 mM in 10 mM sodium acetate buffer, pH 4.5, using the amine coupling kit according to the manufacturer's instructions. Briefly, nearly 900 resonance units (RUs) of the peptide were immobilised under these conditions. The unreacted moieties on the surface were blocked with ethanolamine. All measurements were carried out in 20 mM Tris (pH 7.4), 100 mM NaCl. LPS in running buffer (20 mM Tris, 100 mM NaCl, pH 7.4) flowed over the surface at concentrations of 1, 2, 4, 8, and 16 μg/mL at 25 °C and a flow rate of 10 μL/min. After each injection, the surface was regenerated with 140 μM HAL-2, 50 mM NaOH and 50 mM NaOH containing 0.05% (w/v) SDS. The value of the binding affinity of LPS for HAL-2 was determined using the BIAevaluation 4.1 software (Biacore), selecting the 1:1 Langmuir binding model for the kinetic calculation.

2.8. Thioflavin T fluorescence

Thioflavin T (ThT) has been widely used for the detection of amyloid fibrils because there is a large enhancement of its fluorescence emission when it binds to the cross-β architecture of amyloid. ThT displays excitation maximums (ex) and emission maximums (em) that shift from ~385/445 nm for the free form to ~450/482 nm for the bound form [27]. A stock solution of 10 mM ThT was prepared in Milli-Q water and stored at 4 °C, protected from light to prevent quenching. For ThT fluorescence assays, 150 μL solutions, at pH 7.4 (20 mM Tris, 100 mM NaCl), containing 1 mg/mL LPS and 40–140 μM HAL-2 or its analogues with 47 μM ThT, were incubated in 96-microwell plates (while kept in the dark). A SpectraMax M5 multidetection reader (Molecular Devices

Ltd.) was used to read ThT fluorescence, with excitation at 443 nm and emission at 484 nm. Three replicates corresponding to three wells were measured for each sample to allow for well-to-well variation. All measurements were taken at 20 °C.

The samples for assessment of HAL-2 aggregation induced by *E. coli* were prepared in the same way as for ThT assays, except LPS (1 mg/mL) was replaced with *E. coli* (4×10^8 cfu/mL).

3. Results

3.1. Expression and purification of recombinant ^{15}N-labelled HAL-2

A sequence encoding the HAL-2 peptide was directly introduced into a modified vector pET22b to produce sumo fusion protein (Fig. 1A). For ^{15}N-labelled HAL-2, the recombinant plasmid was overexpressed in *E. coli* BL21(DE3)/pLysS cells grown on minimal M9 medium supplemented with [^{15}N]ammonium chloride. Recombinant HAL-2 was first purified with Ni^{2+}-NTA affinity chromatography, then cleaved with sumo-enzyme, and finally eluted through a C18 semi-preparative column with approximately 40% acetonitrile that contained 0.1% trifluoroacetic acid. The purified HAL-2 was visible as a peptide band approximately 1.4 kDa with slight sumo contaminants, as shown in Tricine-SDS-PAGE (Fig. 1B). This gel fraction was further subjected to molecular weight identification by ESI-MS. The ESI-MS charged ion mass values of $(m + 3H)^+/3$ (1470.78 Da) and $(m + 2H)^+/2$ (1470.56 Da) (Fig. 1C) matched perfectly with the calculated value of 1453.8 Da, combined with the MW increase from the 18 ^{15}N nitrogen isotopes (http://cn.expasy.org/cgi-bin/pi_tool).

3.2. Antimicrobial effects of HAL-2 on E. coli ATCC 25922

HAL-2 has been reported to possess high antimicrobial potency against the two Gram-positive and two Gram-negative bacteria. In the present study, *E. coli* ATCC 25922 was used to study the antimicrobial effects of HAL-2. Three HAL-2 concentrations (20, 40 and 60 μM) were tested for bactericidal activity after incubation at pH 7.4 for 180 min. The kinetics of growth of a culture treated with HAL-2 antibiotic was monitored by the traditional viability counting on agar. As shown in Fig. 2A, the HAL-2 exhibited an obvious dose-dependent antibacterial activity within 180 min. In the first 20 min, the viability of *E. coli*

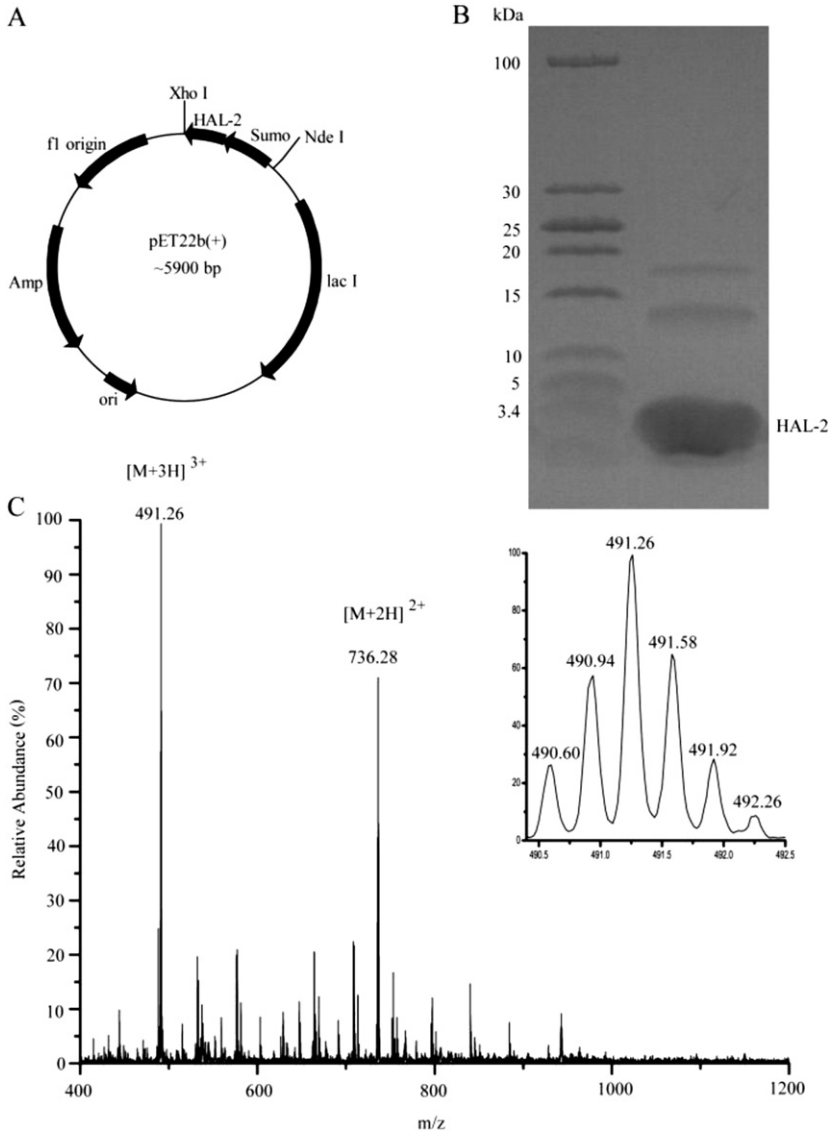

Fig. 1. Cloning, expression and purification of ^{15}N-labelled HAL-2. (A) Schematic diagram of the pET22b expression plasmid; (B) Tricine-SDS-PAGE analysis of HAL-2 after purification; (C) ESI-MS analysis of purified HAL-2 products.

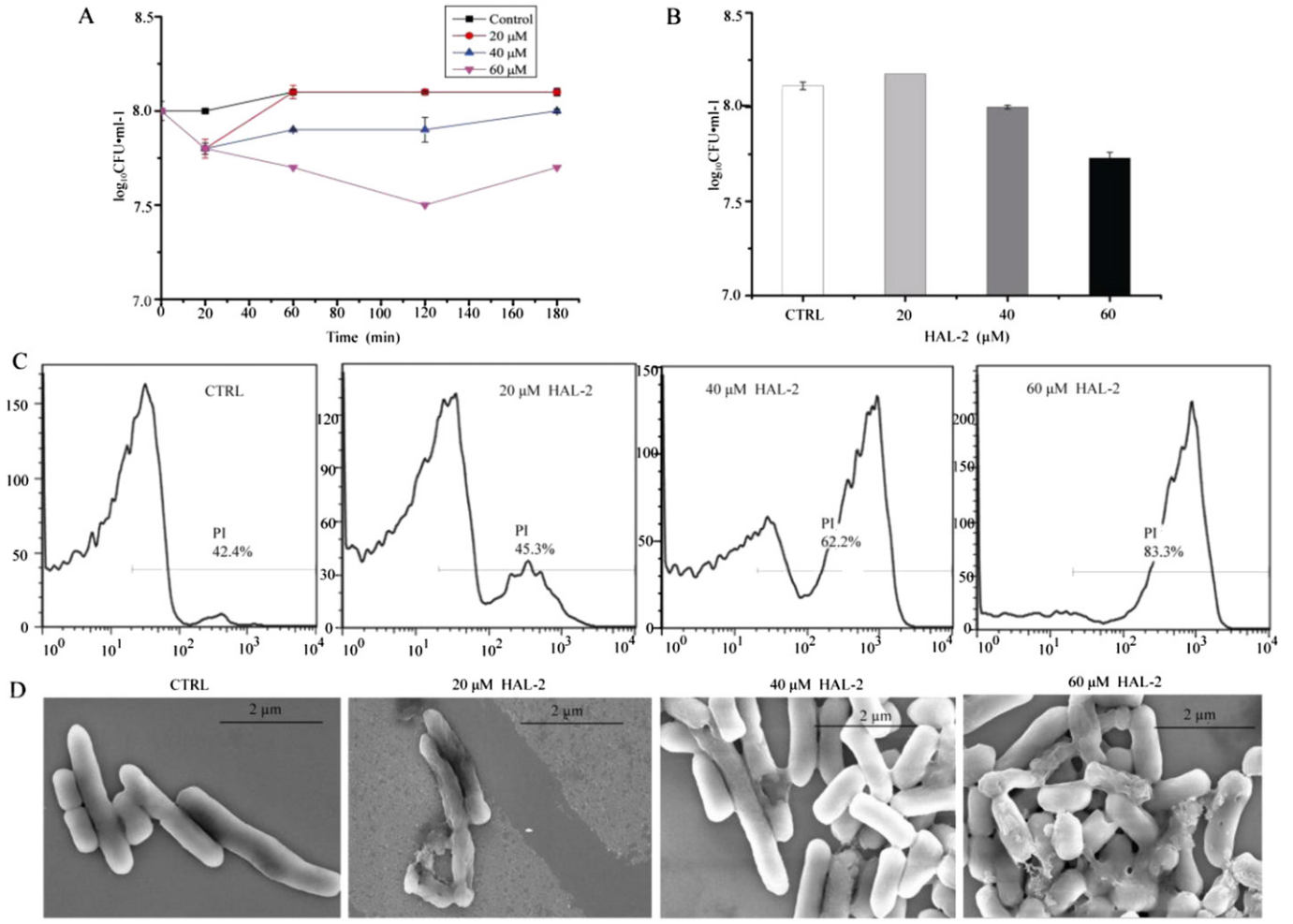

Fig. 2. Bacterial viability of *E. coli* ATCC 25922 after treatment with HAL-2 at pH 7.4. (A) Loss of viability of *E. coli* after incubation with HAL-2. Bacteria were incubated for different incubation times with 20, 40, or 60 μM of HAL-2. Data are the means ± standard deviation of three independent experiments. (B) CFU counts of *E. coli* incubated with 20, 40, or 60 μM of HAL-2 at pH 7.4 for 180 min. (C) Flow cytometry analysis of internalisation of PI by HAL-2 treated *E. coli*. Exponential phase bacterial cells were treated with HAL-2 at pH 7.4, and cellular fluorescence was analysed by flow cytometry. CTRL, without peptide, negative control; HAL-2 was used at concentrations of 20, 40, 60 μM; percentages of PI positive cells are indicated. (D) SEM of HAL-2 treated *E. coli* at pH 7.4. CTRL, control bacteria incubated without peptide; bacteria treated with HAL-2 at concentrations of 20, 40, and 60 μM for up to 180 min are shown.

decreased approximately 0.25 log for all three concentrations of HAL-2. Then, the number of colony-forming units (CFUs) recovered for the *E. coli* incubated with 20 and 40 μM HAL-2. The incubation of *E. coli* with 60 μM of peptide showed a greater antimicrobial activity.

Cell membrane integrity was monitored by assessing the internalisation of a membrane impermeable fluorescent dye, propidium iodide (PI), using flow cytometry. Damage to a cell membrane allows PI, a small cationic molecule, to enter the cell and bind to nucleic acid, thereby providing a rapid detection of antibiotic susceptibility [28]. *E. coli* ATCC 25922 bacterial cells were treated with different concentrations of HAL-2 at pH 7.4 and incubated with PI (5 μg/mL) for 30 min; they were then subjected to flow cytometric analysis. Bacterial cells suspended in buffer and exposed only to PI were used as negative controls. As demonstrated in Fig. 2C, PI positive *E. coli* cells were observed in a significant dose-dependent manner for HAL-2 concentrations of 20 μM (45.3%), 40 μM (62.2%) and 60 μM (83.3%), which agreed with the CFU count results (Fig. 2A and B).

The cell morphology changes by HAL-2 were further characterised by SEM. The images of untreated bacterial cells displayed a smooth bright surface with no apparent cellular debris. In contrast, peptide-exposed cells exhibited a wide range of pronounced morphological change (Fig. 2D). This mainly included deep roughening of the cell surface, the collapse of the cell structure and the loss of bacterial integrity on account of breakage. These phenomena differ from most antimicrobial peptides, which cause blebs on the microbial surface or partial loss of cell content [26,29,30].

3.3. Interactions between HAL-2 and LPS

The secondary structure change of HAL-2 was analysed by CD spectroscopy. In aqueous buffer, the far-UV CD spectrum of HAL-2 showed a strong negative band at 200 nm (Fig. 3A), an indication of a random-coil-like conformation. This is consistent with a previous report that the HAL-2 is unstructured in water [25]. In the presence of LPS, a membrane mimetic environment, HAL-2 disclosed a strong positive band near 195 nm and a negative maximum near 210 nm, suggesting that it can adopt a significant degree of secondary structure (Fig. 3A). More β-sheet (53.3%), rather than the α-helical conformation of native HAL-2, was induced by LPS. This change from a random-coil-like conformation to a folded conformation for HAL-2 is most likely caused by the electrostatic interaction between the positively charged residues in HAL-2 and the negatively charged LPS head group.

To further characterise the HAL-2 and LPS interaction, we utilised the high-resolution ^{31}P NMR technique to study the interaction from the LPS perspective. Because the interaction between the phosphate head groups of LPS and the active peptide HAL-2 causes local chemical environment changes, the ^{31}P chemical shift of the phosphorus atoms in LPS provides an ideal indicator of the mode of interaction. As shown

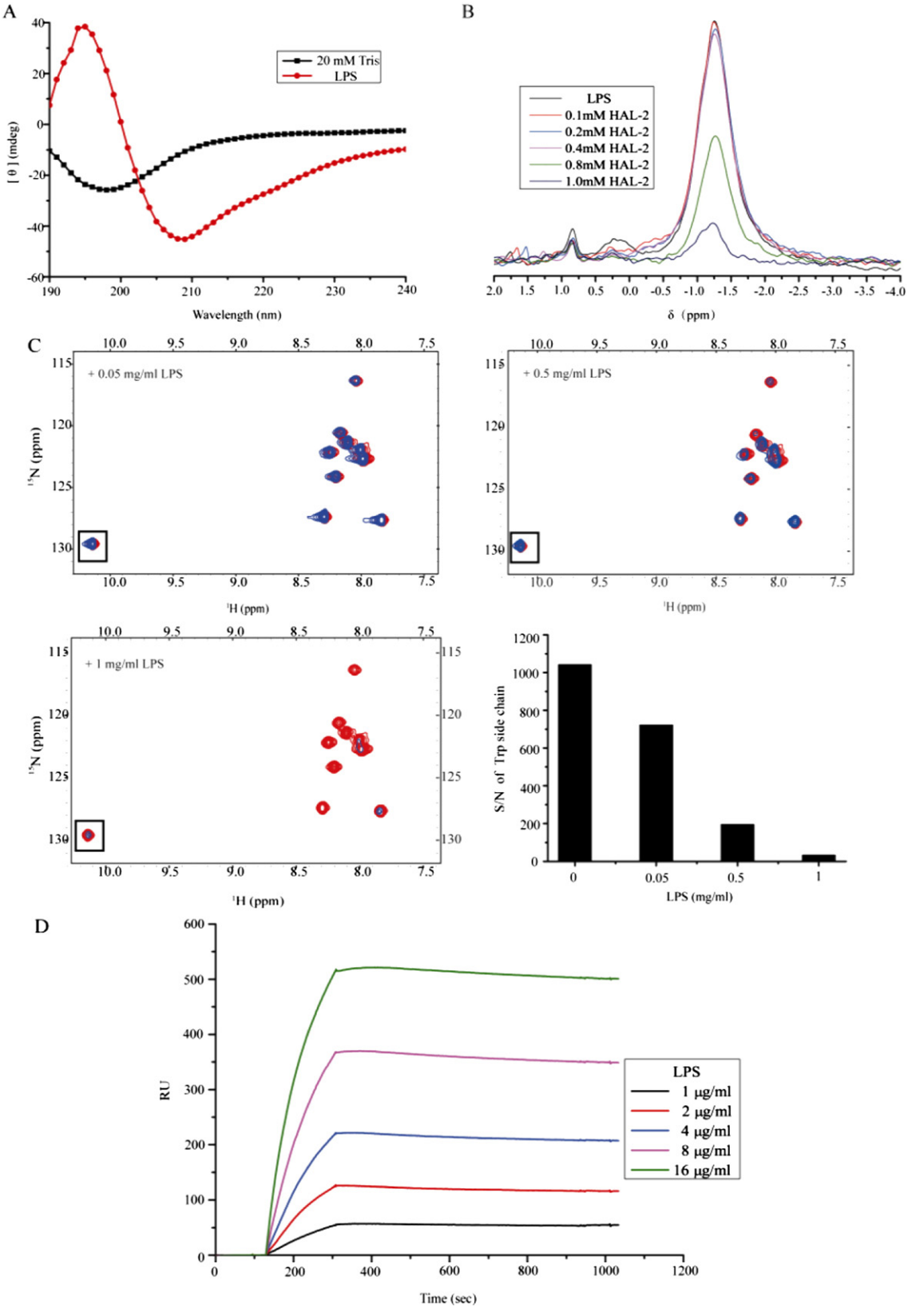

Fig. 3. Interaction of HAL-2 with LPS. (A) Secondary structures of 0.2 mg/mL HAL-2 in the absence and presence of LPS from *E. coli* 055:B5 in 20 mM Tris (pH 7.4) at 298 K. (B) One-dimensional ^{31}P NMR spectra of 4 mg/mL LPS and the spectra after additions of different concentrations of HAL-2 (pH 7.4, 298 K), showing the changes of chemical shifts and the line broadening of the ^{31}P resonances of LPS. (C) HAL-2 bound to LPS in vitro. Overlay of the 2D ^{1}H–^{15}N HSQC spectra of ^{15}N-labelled HAL-2 with 0 (red), 0.05, 0.5 or 1 mg/mL (blue) LPS at pH 7.4. (D) SPR assays of HAL-2 and LPS interaction kinetics. HAL-2 was immobilised on a CM5 sensor chip as ligand, and LPS was diluted in a series of concentrations. Values are recorded in RU for indicated concentrations of LPS.

in Fig. 3B, the ^{31}P resonances of the LPS micelles exhibited a strong peak at −1.30 ppm. As the HAL-2 concentration increased, the LPS ^{31}P spectra changed markedly, indicating a structural perturbation rendered by the peptide (Fig. 3B). First, the LPS micelle peak (−1.30 ppm) experienced a progressive change in line width as a function of increasing concentrations of the HAL-2 peptide, as well as slight chemical shift changes. Changes in the other three peaks also emerged, including a weak peak at about +1.8 ppm, a broad peak around +0.2 ppm, and a sharp peak at about +0.8 ppm. The signal at +1.8 ppm shifted upfield as the HAL-2 concentration increased, and it disappeared in the presence of 0.8 mM HAL-2. Conversely, intensity changes were observed for the sharp peak at +0.8 ppm and the broad peak at +0.2 ppm. The dramatic line broadening of ^{31}P resonances (−1.30 ppm) of LPS after binding to HAL-2 indicated a restricted mobility of the phosphate groups, which could be due to either larger micelle formations and/or conformational exchanges among different states of peptide–LPS complexes. Furthermore, the upfield shift of the ^{31}P resonance at +1.8 ppm suggested that the chemical environment and/or conformation of some of the phosphates had changed. Taken together, these data confirmed that LPS provides interaction sites for the cationic peptide and LPS micelles undergo structural changes when complexed with HAL-2.

Further NMR experiments were conducted to characterise the interaction from the HAL-2 perspective. HSQC spectra were recorded on a ^{15}N-labelled HAL-2 sample (1 mM, in 95% buffer, 5% D2O at pH 7.4, 25 °C) with or without LPS (0.05, 0.5 or 1 mg/mL) (Fig. 3C). At 0.05 mg/mL LPS, no obvious spectral change was observed. HAL-2 signals started to decrease when the LPS concentration reached 0.5 mg/mL, and two peaks (8.04 ppm/116 ppm; 8.165 ppm/120 ppm) almost vanished. When 1 mg/mL LPS was added, the majority of the peaks disappeared in the HSQC spectrum of HAL-2. As exemplified by the changes of Trp side chain signal, the addition of LPS reduced the amount of free HAL-2, implying the binding of HAL-2 to LPS micelles and the formation of a large complex (Fig. 3C).

We also used SPR spectroscopy to investigate the relationship between HAL-2 and LPS. As illustrated in Fig. 3D, a typical sensorgram for the binding of the varying concentrations of LPS to HAL-2 is shown. A rapid enhancement of the RUs of LPS binding to immobilised HAL-2 demonstrated the direct interaction between HAL-2 and LPS, and the binding of LPS as analyte to HAL-2 as ligand exhibited a dose-dependent pattern at concentrations of 1–16 μg/mL. Kinetic analysis for the interaction of HAL-2 with LPS yielded a mean value of $K_D = 1.31 \times 10^{-8}$ M, indicating an evident affinity between HAL-2 and LPS.

3.4. Aggregation mode in the interaction of LPS and HAL-2

LPS is the major component of the outer membrane of Gram-negative bacteria and has been thought to evolve for protection of bacteria against antibacterial molecules. Many AMPs show antimicrobial activity because of their LPS-neutralising properties. We monitored the interaction mode between HAL-2 and LPS (Fig. 4A) or *E. coli* (Fig. 4B) with the ThT fluorescence. Aggregation occurred once LPS or *E. coli* was added, and this aggregation activity depended on the peptide concentrations, indicating a nucleation-dependent aggregation process. At the same time, LPS and *E. coli* showed aggregation in the interaction with HAL-2. The aggregation in this reaction mixture might exist as either an intermolecular electrostatic interaction or an intramolecular one.

3.5. Less amyloid formation and antimicrobial activity of HAL-2 mutants

To further investigate the relationship between amyloid formation and the antimicrobial activity of HAL-2, we constructed three HAL-2 analogues, HAL-2L6(D), HAL-2K8P and HAL-2H9P. The CD experiments were carried out to determine the secondary structure of HAL-2 analogues (Fig. 5A). Similar to HAL-2, the analogues had random conformations in free solution and showed a marked ability to adopt largely β-sheet structures in the presence of hydrophobic LPS, containing approximately 53.8% (HAL-2L6(D)), 56.9% (HAL-2K8P), 59.7% (HAL-2H9P) of β-sheet structure. Furthermore, the formation of amyloid aggregates was also checked by ThT fluorescence. As illustrated in Fig. 5B, the analogues incubated in LPS underwent amyloid aggregation, which was peptide concentration dependent. However, reductions of ThT intensity were observed at all concentrations of the peptide analogues, compared with HAL-2. The inhibition of *E. coli* by the HAL-2 analogues was further investigated by assessing cell viability loss within 180 min at pH 7.4. Compared with HAL-2, the analogues caused almost no reduction in the number of CFU (Fig. 5C). These observations indicated that the mutations affected the ability of the amyloid formation of the HAL-2 analogues and thus lowered the antimicrobial activity.

4. Discussion

HAL-2, which is among the shortest linear cationic AMPs found in nature, was first isolated from the venom of the eusocial bee *H. sexcinctus*, and it has been reported to display a broad spectrum of antimicrobial activity against bacteria, fungi or several types of cancer cells [25]. Bacterial viability counting showed that HAL-2 exhibited an

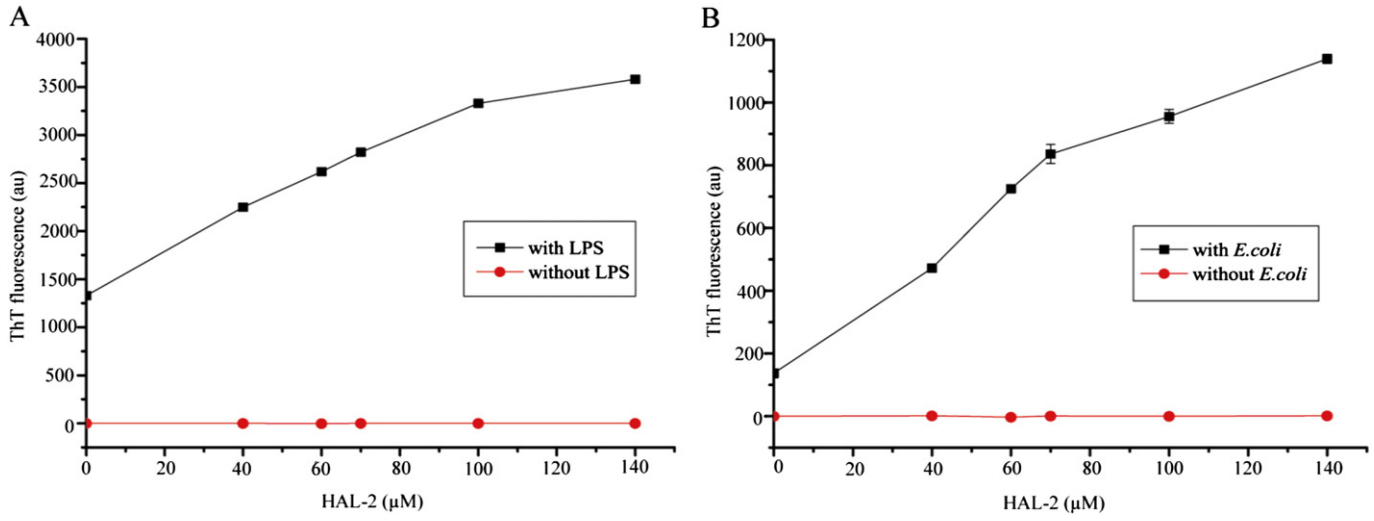

Fig. 4. Aggregate formation in the interaction between HAL-2 and LPS (A) or HAL-2 and *E. coli* (B) at pH 7.4. LPS (1 mg/mL) or *E. coli* (4×10^8 cfu/mL) in the absence and presence of different concentrations of HAL-2, as monitored by ThT fluorescence. The concentrations of the peptide were 40, 60, 70, 100, and 140 μM, and ThT was 47 μM.

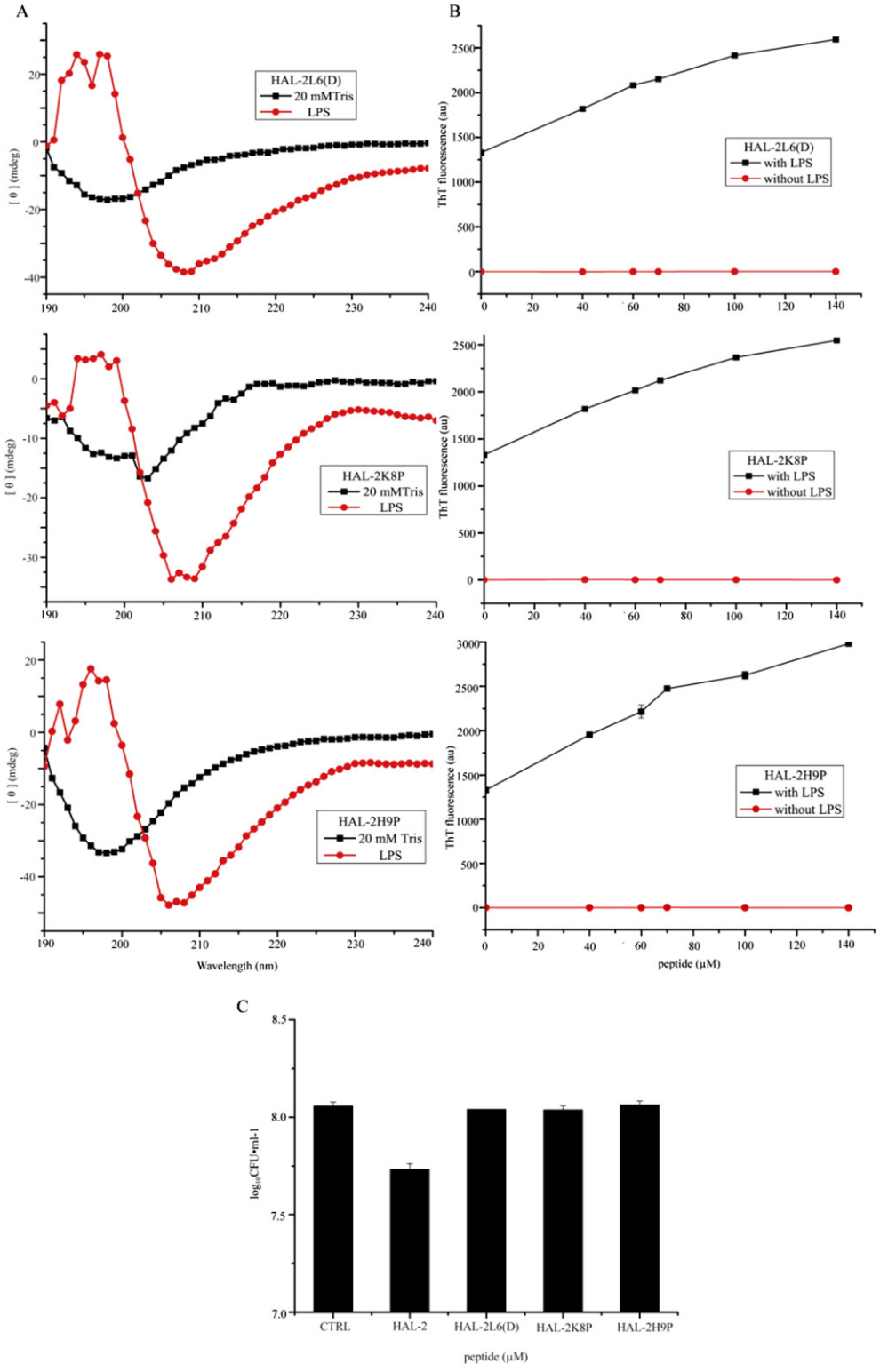

Fig. 5. Relationship between amyloid formation and antimicrobial activity. (A) CD spectra of peptides (0.2 mg/mL in 20 mM Tris, pH 7.4) in the absence and presence of 2 mg/mL LPS; (B) peptide amyloid formation measured by ThT fluorescence emission; (C) the comparison of antimicrobial activity between HAL-2 and its analogues at 180 min.

obvious dose-dependent antibacterial activity within 3 h (Fig. 2A). We used propidium iodide (PI) and flow cytometry to assess the membrane integrity of *E. coli* ATCC 25922 after treatment with HAL-2; the results showed that HAL-2 was able to break *E. coli* membranes, leading to the staining of DNA by the PI dye (Fig. 2C). The peptide-exposed bacterial cells exhibited a wide range of pronounced changes in their morphology, as demonstrated by the SEM images, while untreated bacterial cells displayed a smooth bright surface with no apparent cellular debris (Fig. 2D).

Gram-negative bacteria have a cell wall that is rich in acidic lipids such as LPS and a central peptidoglycan layer, which forms a permeability barrier that must be overcome by broad-spectrum AMPs. Many reports have analysed the structures of AMPs in the presence of LPS or mimetic membranes of Gram-negative bacteria to understand the

mechanism of LPS or lipid-membrane recognition by AMPs [31–33]. However, the details of the interaction between AMPs and LPS and the relationship between the mechanisms of LPS recognition and structures of AMPs have not yet been revealed. HAL-2 possesses four basic residues at pH 7.4, leading to a cationic +4 global charge, so a preferred interaction with the anionic lipid is probable. HAL-2 also contains a histidine residue in the amino acid sequence. It has been suggested that at pH values below the pKa of the histidine groups (pKa 6.5), histidine residues may be protonated, resulting in an increase in the positive net charge of the corresponding peptide. Hepcidin, a histidine containing AMP, has been reported to have a pH-dependent antimicrobial activity [29]. In fact, a stronger effect on *E. coli* was observed at pH 5.0 (data not shown), suggesting a different mode of LPS interaction. This electrostatic interaction between the positively charged residues in HAL-2 and the negatively charged lipid may contribute to the recruitment of HAL-2 to the bacterial surface and to the conformational changes for HAL-2 upon lipid binding.

To study the secondary structure of HAL-2 in the absence and presence of LPS, we performed CD spectroscopy. HAL-2 that was freshly dissolved in 20 mM Tris buffer with LPS displayed a peak with negative ellipticity at approximately 210 nm and a peak with positive ellipticity at 195 nm, peaks that are characteristic of β-sheet structures (Fig. 3A). Deconvolution of this spectrum estimated the proportion of secondary structures to be 15.5% α-helix, 53.3% β-sheet, 6.7% turn and 24.5% random coil. In TFE/water mixtures, CD experiments (data not shown) showed that HAL-2 folds into an α-helical structure. This is consistent with a previous report that HAL-2 forms an α-helical structure in the presence of TFE or SDS, and an amphipathic helical model has been proposed where the hydrophilic amino acid residues are situated on one side of the α-helix and the hydrophobic amino acid residues are on the opposite side. However, when HAL-2 is in the presence of LPS, more β-sheet (53.3%) conformation, compared with α-helical conformation, is induced. This finding was further confirmed by the ThT experiments, where the fluorescent dye ThT bound to fibrils, indicating the aggregation of the amyloidogenic proteins. The ThT fluorescence intensity increased when LPS or *E. coli* was added to the peptides, or when the peptides were added to LPS or *E. coli*, although LPS or *E. coli* alone also exhibited ThT fluorescence (Fig. 4). Taken together, these results suggest that LPS or *E. coli* could induce the amyloid aggregation of HAL-2, which leads to secondary structure changes of HAL-2 (Fig. 3A).

LPS covers >70% of the outer leaflet of Gram-negative bacteria [34], and the antimicrobial peptides have to transverse this outer membrane and reach the inner phospholipid layer to promote bacterial death. A previous study suggested an “AMP trap” model, in which LPS induces the peptide to form a bulky compound that is unable to insert into the microbial membrane, effectively inactivating the peptide with a minimal inhibitory concentration of approximately 100 μM. The incorporation of D-amino acids can overcome this “trapping” mechanism by preventing the formation of oligomers, which allows the peptide to traverse through the LPS outer membrane. The corresponding minimal inhibitory concentration was lowered to 5 μM [35]. In this study, we found that once HAL-2 interacted with LPS, peptide aggregation was triggered and amyloid was formed. As the peptide concentration increased, more amyloid formed (Fig. 4) and a greater loss of bacterial viability was observed (Fig. 2), indicating a positive correlation between the amyloid formation and the antimicrobial activity of HAL-2. As shown in Fig. 2A, the effective antimicrobial concentration of HAL-2 peptide is below 20 μM, which is significantly lower than that of “AMP trap” peptide. For the HAL-2 analogues, less amyloid aggregation formed in the presence of LPS, and most of the antimicrobial activity was lost, compared with the wild type HAL-2 peptide. These observations provide strong evidence that amyloid formation is indeed essential for the antimicrobial activity of HAL-2.

A similar amyloid forming property has been studied in vitro for other antimicrobial peptides in the presence of lipid membranes [36–39], and a “leaky slit” model was proposed based on amyloid formation by AMPs on the membrane surface [40]. These studies were limited to artificial lipid membranes, so the effect of AMP amyloid with LPS, which forms the bacterial cell wall barrier, has not been discussed. Interestingly, some amyloid peptides that are known for their close relevance to human diseases, including type II diabetes [41], Creutzfeldt–Jakob disease [42], and Abeta of Alzheimer's disease [43], have also been found to have antimicrobial activities that normally function in the innate immune system in response to infections. We speculate that amyloid aggregation may lead to the toxicity and the antimicrobial activity of some peptides, possibly as the result of the binding of the peptide in an aggregated state, but as yet unknown factors regulate that specific binding and aggregation.

The interaction between HAL-2 and LPS is very complicated, and questions of how the negatively charged LPS surface induces amyloid formation and how the HAL-2 amyloid causes cell leakage remain to be elucidated. In our experiments, HAL-2 was confirmed to interact with LPS by SPR data (Fig. 3D), and a strong interaction between them was observed (washing with 140 μM HAL-2 was necessary to thoroughly regenerate the sensor chip), yielding a value of $K_D = 1.31 \times 10^{-8}$ M. An isothermal titration calorimetry (ITC) experiment was also performed to investigate the binding of HAL-2 to LPS (data not shown), but an accurate binding constant could not be extracted from the obtained titration curves; multiple factors may contribute to the enthalpy of binding of the peptides to LPS, as reported in a similar system [44]. Moreover, ^{1}H–^{15}N HSQC and ^{31}P experiments were performed to characterise HAL-2 and LPS interaction from both peptide and lipid perspective. The line-broadening of HAL-2 HSQC resonances and an LPS ^{31}P peak at −1.30 ppm suggest the formation of HAL-2/LPS complexes (Fig. 3B and C). The changes emerging from multiple ^{31}P peaks (−1.3 ppm, +1.8 ppm, +0.2 ppm, and +0.8 ppm) upon HAL-2 binding indicate that the phosphate head groups of LPS within the sample experienced various local chemical environments. Due to the complexity of LPS ^{31}P spectra upon HAL-2 binding, we were not able to trace the ^{31}P resonance assignments and analyse the interaction details. Moreover, the behaviour of these resonances varied as the HAL-2 concentration increased, including line broadening, signal disappearance and frequency shifts, indicating complex structural and dynamic differences in the lipid molecules. The heterogeneity associated with LPS compositions, which is not demonstrated in the LPS only spectrum, may contribute to the complex phase and dynamics behaviours of LPS upon HAL-2 binding.

In conclusion, this study sheds light on several clues regarding the molecular mechanism of the antimicrobial peptide HAL-2. After electrostatically binding to LPS, HAL-2 adopts a β-strand conformation and consequently forms amyloid aggregates. Importantly, this amyloid state makes it possible for the HAL-2 to traverse through the LPS outer membrane and disrupt the integrity of the inner membrane (Fig. 2C). However, the incorporation of D-amino acid and proline substitutions can prevent its antimicrobial activity, and less amyloid aggregation occurs. We propose that the aggregation state may play an important role in HAL-2 antimicrobial activity. Overall, this study increases our understanding of the molecular basis of the antimicrobial activity mediated by LPS, and it could provide information to design novel antimicrobial peptides for future therapeutic purposes.

Acknowledgements

This work was supported by Natural Science Foundation of China (Grants 21372222 and 21103199), and Hefei Center for Physical Science and Technology.

References

[1] J. Verhoef, Antibiotic resistance: the pandemic, Adv. Exp. Med. Biol. 531 (2003) 301–313.
[2] H.C. Neu, The crisis in antibiotic resistance, Science 257 (1992) 1064–1073.

[3] M. Zasloff, Antimicrobial peptides of multicellular organisms, Nature 415 (2002) 389–395.
[4] A. Tossi, L. Sandri, A. Giangaspero, Amphipathic, α-helical antimicrobial peptides, Pept. Sci. 55 (2000) 4–30.
[5] P. Bulet, R. Stöcklin, L. Menin, Anti-microbial peptides: from invertebrates to vertebrates, Immunol. Rev. 198 (2004) 169–184.
[6] R. Danesi, S. Senesi, J.W.v.t. Wout, J.T.v. Dissel, A. Lupetti, P.H. Nibbering, Antimicrobial peptides: therapeutic potential for the treatment of *Candida* infections, Expert Opin. Investig. Drugs 11 (2002) 309–318.
[7] Y.J. Gordon, E.G. Romanowski, A.M. McDermott, A review of antimicrobial peptides and their therapeutic potential as anti-infective drugs, Curr. Eye Res. 30 (2005) 505–515.
[8] R.E.W. Hancock, H.G. Sahl, Antimicrobial and host-defense peptides as new anti-infective therapeutic strategies, Nat. Biotechnol. 24 (2006) 1551–1557.
[9] L. Zhang, T.J. Falla, Antimicrobial peptides: therapeutic potential, Expert. Opin. Pharmacother. 7 (2006) 653–663.
[10] K.A. Brogden, Antimicrobial peptides: pore formers or metabolic inhibitors in bacteria? Nat. Rev. Microbiol. 3 (2005) 238–250.
[11] M. Pushpanathan, P. Gunasekaran, J. Rajendhran, Antimicrobial peptides: versatile biological properties, Int. J. Pept. 2013 (2013) 675391.
[12] B.M. Peters, M.E. Shirtliff, M.A. Jabra-Rizk, Antimicrobial peptides: primeval molecules or future drugs? PLoS Pathog. 6 (2010) e1001067.
[13] M. Dathe, T. Wieprecht, Structural features of helical antimicrobial peptides: their potential to modulate activity on model membranes and biological cells, Bba—Biomembranes 1462 (1999) 71–87.
[14] L. Zhang, A. Rozek, R.E. Hancock, Interaction of cationic antimicrobial peptides with model membranes, J. Biol. Chem. 276 (2001) 35714–35722.
[15] V. Teixeira, M.J. Feio, M. Bastos, Role of lipids in the interaction of antimicrobial peptides with membranes, Prog. Lipid Res. 51 (2012) 149–177.
[16] S. Galdiero, A. Falanga, M. Cantisani, M. Vitiello, G. Morelli, M. Galdiero, Peptide–lipid interactions: experiments and applications, Int. J. Mol. Sci. 14 (2013) 18758–18789.
[17] J.A. Yethon, C. Whitfield, Lipopolysaccharide as a target for the development of novel therapeutics in gram-negative bacteria, Curr. Drug Targets Infect. Disord. 1 (2001) 91–106.
[18] L. Ding, L. Yang, T.M. Weiss, A.J. Waring, R.I. Lehrer, H.W. Huang, Interaction of antimicrobial peptides with lipopolysaccharides, Biochemistry 42 (2003) 12251–12259.
[19] M.G. Scott, A.C. Vreugdenhil, W.A. Buurman, R.E. Hancock, M.R. Gold, Cutting edge: cationic antimicrobial peptides block the binding of lipopolysaccharide (LPS) to LPS binding protein, J. Immunol. 164 (2000) 549–553.
[20] M.G. Scott, D.J. Davidson, M.R. Gold, D. Bowdish, R.E.W. Hancock, The human antimicrobial peptide LL-37 is a multifunctional modulator of innate immune responses, J. Immunol. 169 (2002) 3883–3891.
[21] X.X. Guo, C.B. Ma, Q. Du, R. Wei, L. Wang, M. Zhou, et al., Two peptides, TsAP-1 and TsAP-2, from the venom of the Brazilian yellow scorpion, *Tityus serrulatus*: evaluation of their antimicrobial and anticancer activities, Biochimie 95 (2013) 1784–1794.
[22] L. Kuhn-Nentwig, J. Muller, J. Schaller, A. Walz, M. Dathe, W. Nentwig, Cupiennin 1, a new family of highly basic antimicrobial peptides in the venom of the spider *Cupiennius salei* (Ctenidae), J. Biol. Chem. 277 (2002) 11208–11216.
[23] L. Monincova, J. Slaninova, V. Fucik, O. Hovorka, Z. Voburka, L. Bednarova, et al., Lasiocepsin, a novel cyclic antimicrobial peptide from the venom of eusocial bee *Lasioglossum laticeps* (Hymenoptera: Halictidae), Amino Acids 43 (2012) 751–761.
[24] N.G. de Oliveira, M.H.E.S. Cardoso, O.L. Franco, Snake venoms: attractive antimicrobial proteinaceous compounds for therapeutic purposes, Cell. Mol. Life Sci. 70 (2013) 4645–4658.
[25] L. Monincova, M. Budesinsky, J. Slaninova, O. Hovorka, J. Cvacka, Z. Voburka, et al., Novel antimicrobial peptides from the venom of the eusocial bee *Halictus sexcinctus* (Hymenoptera: Halictidae) and their analogs, Amino Acids 39 (2010) 763–775.
[26] L. Wei, J.J. Yang, X.Q. He, G.X. Mo, J. Hong, X.W. Yan, et al., Structure and function of a potent lipopolysaccharide—binding antimicrobial and anti-inflammatory peptide, J. Med. Chem. 56 (2013) 3546–3556.
[27] M. Biancalana, S. Koide, Molecular mechanism of Thioflavin-T binding to amyloid fibrils, Bba—Proteins Proteom 1804 (2010) 1405–1412.
[28] V.A. Gant, G. Warnes, I. Phillips, G.F. Savidge, The application of flow-cytometry to the study of bacterial responses to antibiotics, J. Med. Microbiol. 39 (1993) 147–154.
[29] G. Maisetta, A. Vitali, M.A. Scorciapino, A.C. Rinaldi, R. Petruzzelli, F.L. Brancatisano, et al., pH-dependent disruption of *Escherichia coli* ATCC 25922 and model membranes by the human antimicrobial peptides hepcidin 20 and 25, FEBS J. 280 (2013) 2842–2854.
[30] M. Torrent, B.G. de la Torre, V.M. Nogues, D. Andreu, E. Boix, Bactericidal and membrane disruption activities of the eosinophil cationic protein are largely retained in an N-terminal fragment, Biochem. J. 421 (2009) 425–434.
[31] P.N. Domadia, A. Bhunia, A. Ramamoorthy, S. Bhattacharjya, Structure, interactions, and antibacterial activities of MSI-594 derived mutant peptide MSI-594F5A in Lipopolysaccharide micelles: role of the helical hairpin conformation in outer-membrane permeabilization, J. Am. Chem. Soc. 132 (2010) 18417–18428.
[32] A. Bhunia, P.N. Domadia, J. Torres, K.J. Hallock, A. Ramamoorthy, S. Bhattacharjya, NMR structure of pardaxin, a pore-forming antimicrobial peptide, in lipopolysaccharide micelles mechanism of outer membrane permeabilization, J. Biol. Chem. 285 (2010) 3883–3895.
[33] T. Kushibiki, M. Kamiya, T. Aizawa, Y. Kumaki, T. Kikukawa, M. Mizuguchi, et al., Interaction between tachyplesin I, an antimicrobial peptide derived from horseshoe crab, and lipopolysaccharide, Bba—Proteins Proteom 1844 (2014) 527–534.
[34] A. Schmidtchen, M. Malmsten, Peptide interactions with bacterial lipopolysaccharides, Curr. Opin. Colloid Interface Sci. 18 (2013) 381–392.
[35] N. Papo, Y. Shai, A molecular mechanism for lipopolysaccharide protection of gram-negative bacteria from antimicrobial peptides, J. Biol. Chem. 280 (2005) 10378–10387.
[36] H.X. Zhao, E.K.J. Tuominen, P.K.J. Kinnunen, Formation of amyloid fibers triggered by phosphatidylserine-containing membranes, Biochemistry 43 (2004) 10302–10307.
[37] R. Sood, Y. Domanov, P.K.J. Kinnunen, Fluorescent temporin B derivative and its binding to liposomes, J. Fluoresc. 17 (2007) 223–234.
[38] R. Sood, Y. Domanov, M. Pietiainen, V.P. Kontinen, P.K.J. Kinnunen, Binding of LL-37 to model biomembranes: insight into target vs host cell recognition, Bba—Biomembranes 1778 (2008) 983–996.
[39] L. Caillon, J.A. Killian, O. Lequin, L. Khemtemourian, Biophysical investigation of the membrane-disrupting mechanism of the antimicrobial and amyloid-like peptide dermaseptin S9, PLoS One 8 (2013).
[40] H. Zhao, R. Sood, A. Jutila, S. Bose, G. Fimland, J. Nissen-Meyer, et al., Interaction of the antimicrobial peptide pheromone Plantaricin A with model membranes: implications for a novel mechanism of action, Bba—Biomembranes 1758 (2006) 1461–1474.
[41] L. Wang, Q. Liu, J.C. Chen, Y.X. Cui, B. Zhou, Y.X. Chen, et al., Antimicrobial activity of human islet amyloid polypeptides: an insight into amyloid peptides' connection with antimicrobial peptides, Biol. Chem. 393 (2012) 641–646.
[42] M. Pasupuleti, M. Roupe, V. Rydengard, K. Surewicz, W.K. Surewicz, A. Chalupka, et al., Antimicrobial activity of human prion protein is mediated by its N-terminal region, PLoS One 4 (2009).
[43] S.J. Soscia, J.E. Kirby, K.J. Washicosky, S.M. Tucker, M. Ingelsson, B. Hyman, et al., The Alzheimer's disease-associated amyloid beta-protein is an antimicrobial peptide, PLoS One 5 (2010).
[44] R.F. Epand, W.L. Maloy, A. Ramamoorthy, R.M. Epand, Probing the "charge cluster mechanism" in amphipathic helical cationic antimicrobial peptides, Biochemistry 49 (2010) 4076–4084.